

Supporting Information

The Role of Blend Ratio in Polymer:Fullerene Phototransistors

Cintha Trujillo Herrera,¹ Min Ji Hong,¹ John G. Labram^{1}*

¹School of Electrical Engineering and Computer Science, Oregon State University, Corvallis,
Oregon 97331, USA

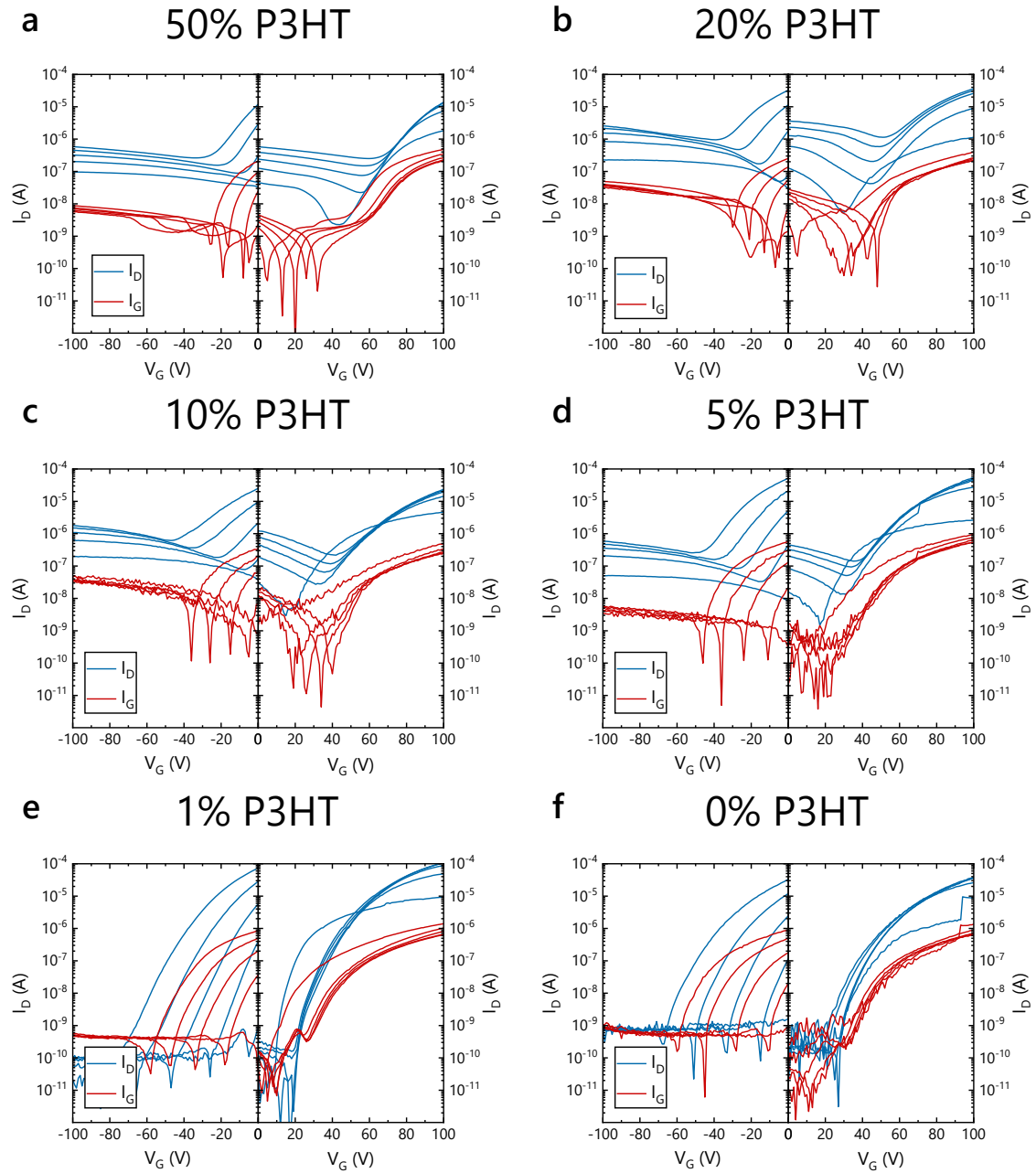
Corresponding Author

*Email: john.labram@oregonstate.edu

Table of Contents

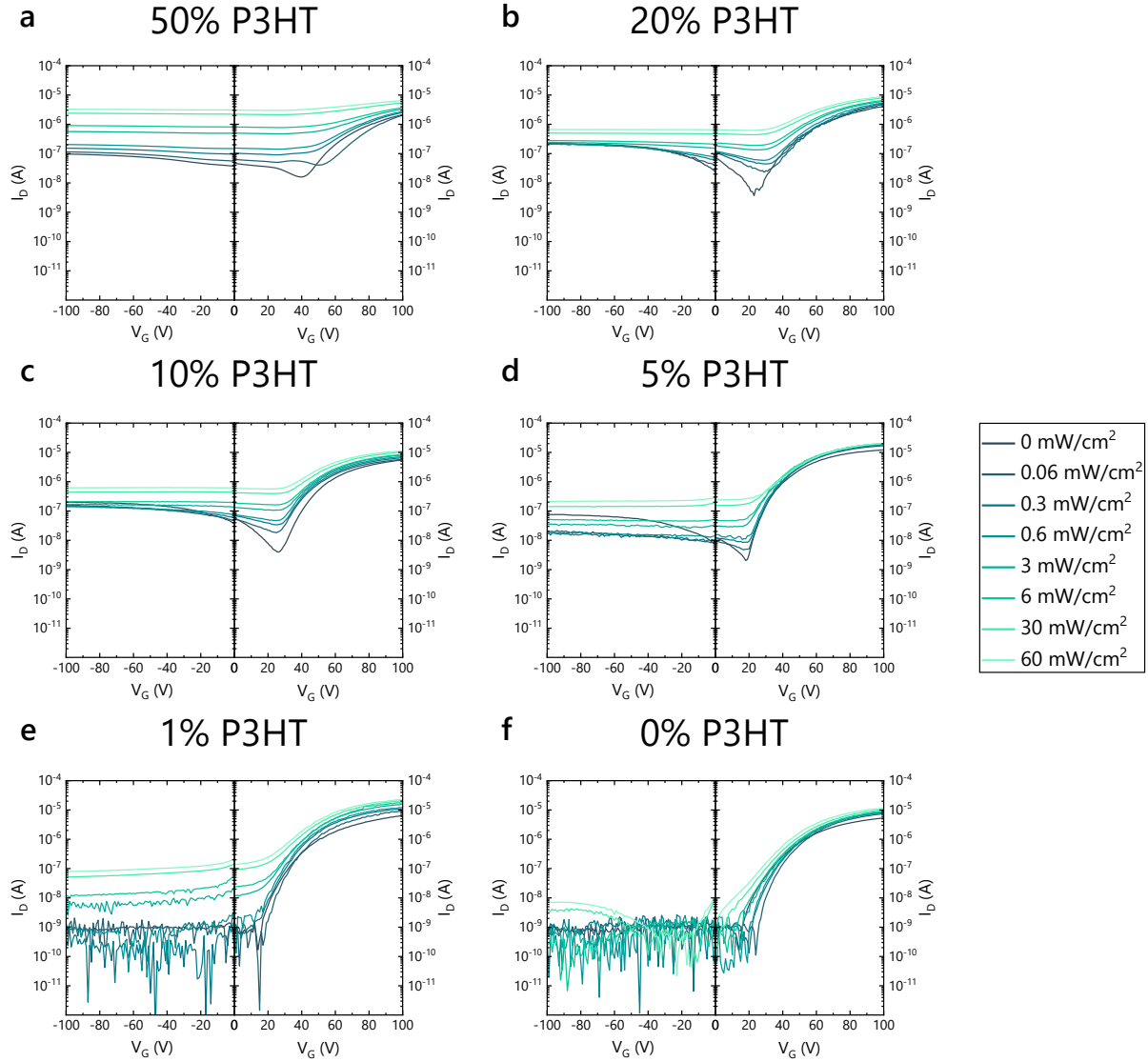
S1. Transfer Characteristics in the Dark	2
S2. Transfer Characteristics under Illumination	3
S3. Photocurrent	4
S4. Responsivity	5
S5. External Quantum Efficiency	6
S6. Change in Threshold Voltage under Illumination	7
S7. Ratio of Photocurrent to Dark Current	8
S8. Time-Resolved Microwave Conductivity (TRMC) Data	9
Supporting References	11

S1. Transfer Characteristics in the Dark



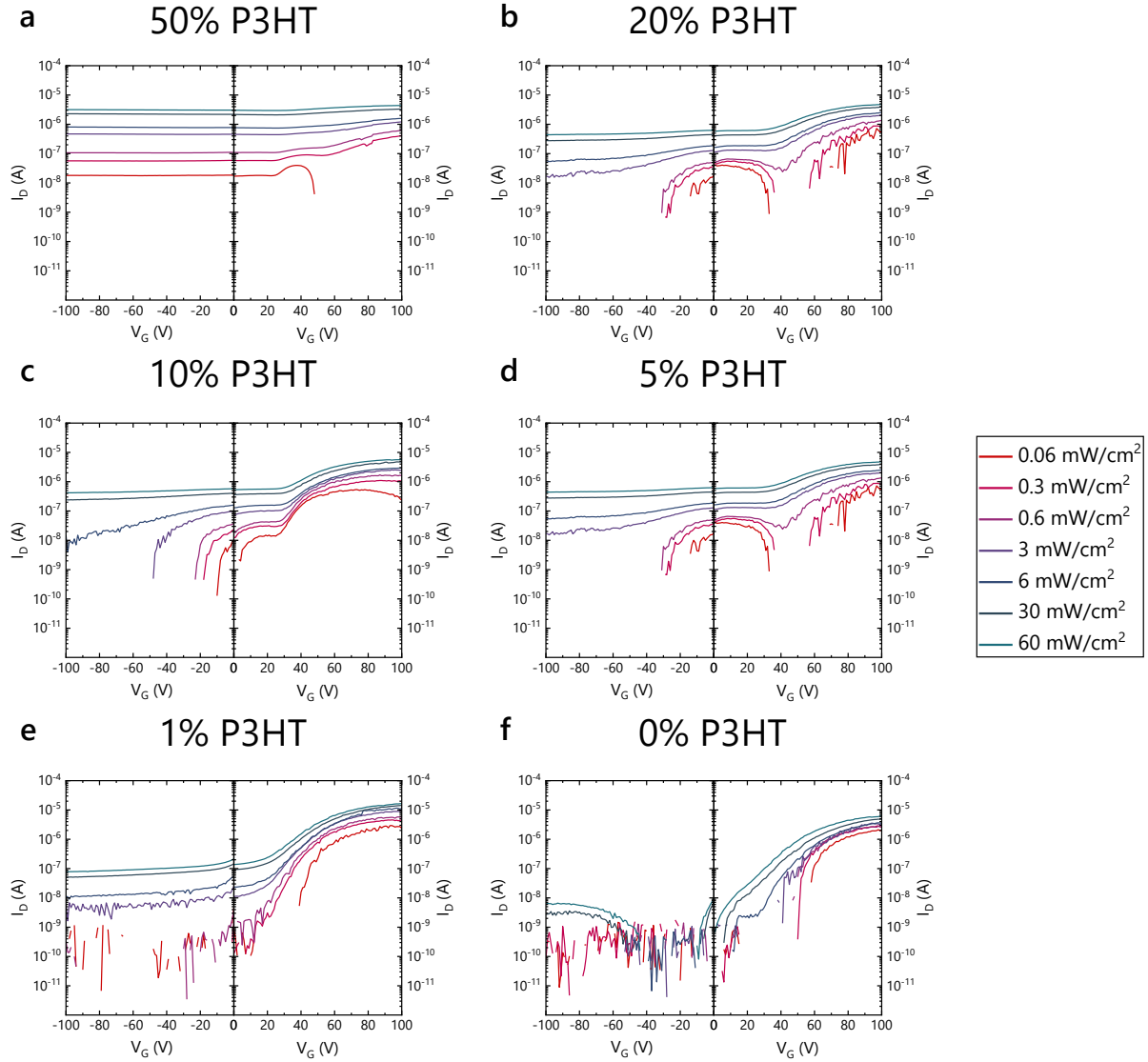
Supplementary Figure S1 p-Type (left) and n-Type (right) transfer characteristics (source-drain current, I_D , as a function of gate voltage, V_G) of poly(3-hexylthiophene-2,5-diyl) (P3HT) and phenyl-C₆₁-butyric acid methyl ester (PCBM) blend thin-film transistors (TFT) measured in the dark. The weight % of P3HT was **a** 50%, **b** 20%, **c** 10%, **d** 5%, **e** 1%, **f** 0%. Source-drain current (I_D) is shown in blue and gate leakage current (I_G) is shown in red. Each device has a channel length of 20 μm , a channel width of 1 cm, and a dielectric capacitance of 15 nF/cm². Each line is a measurement carried out at a different drain voltage (V_D) between $V_D = -20\text{V}$ and -100V for p-type measurements and $V_D = 20\text{V}$ and 100V for n-type measurements. Devices were measured under atmospheric pressure N₂ at room temperature. All TFTs measured were in the bottom-gate, bottom-contact (BGBC) architecture, as shown in Figure 1a of the main text.

S2. Transfer Characteristics under Illumination



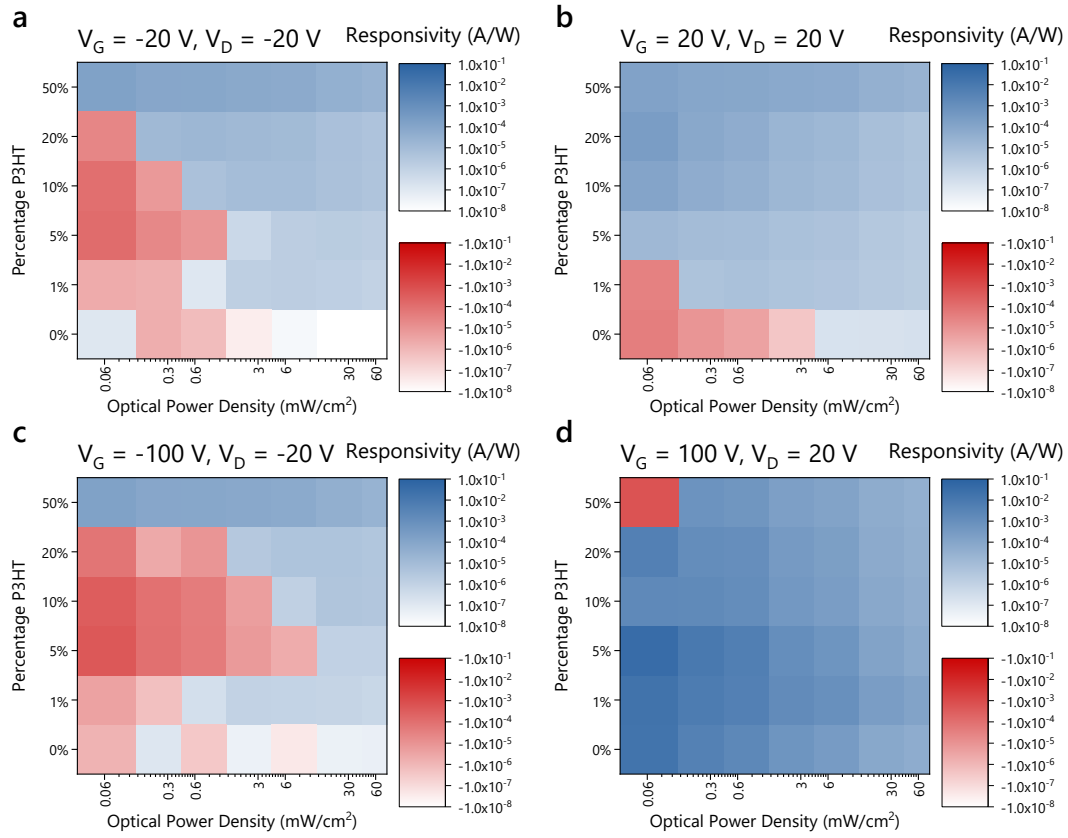
Supplementary Figure S2 p-Type (left) and n-Type (right) transfer characteristics (source-drain current, I_D , as a function of gate voltage, V_G) for thin film transistors (TFTs) formed of blends of poly(3-hexylthiophene-2,5-diyl) (P3HT) and phenyl-C₆₁-butyric acid methyl ester (PCBM), measured under various intensities of green ($\lambda_{\text{max}} = 525$ nm) light. The weight % of P3HT was **a** 50%, **b** 20%, **c** 10%, **d** 5%, **e** 1%, **f** 0%. All TFTs measured were in the bottom-gate, bottom-contact (BGBC) architecture, as shown in Figure 1a of the main text. All devices had a channel length of 20 μm , a channel width of 1 cm, and a dielectric capacitance of 15 nF/cm^2 . Drain voltages of $V_D = -20$ V were applied for negative V_G (left panels) and $V_D = +20$ V, were applied for positive V_G (right panels). All devices were measured under atmospheric pressure N_2 at room temperature. Legend shows incident optical power density.

S3. Photocurrent



Supplementary Figure S3 p-Type (left) and n-Type (right) photocurrent ($I_{ph} = I_D^{(illuminated)} - I_D^{(dark)}$) for thin film transistors (TFTs) formed of blends of poly(3-hexylthiophene-2,5-diyl) (P3HT) and phenyl-C₆₁-butyric acid methyl ester (PCBM), measured under various intensities of green ($\lambda_{max} = 525$ nm) light. The weight % of P3HT was **a** 50%, **b** 20%, **c** 10%, **d** 5%, **e** 1%, **f** 0%. Negative values of I_{ph} are not displayed. All TFTs measured were in the bottom-gate, bottom-contact (BGBC) architecture, as shown in Figure 1a of the main text. All devices had a channel length of 20 μ m, a channel width of 1 cm, and a dielectric capacitance of 15 nF/cm². Drain voltages of $V_D = -20$ V were applied for negative V_G (left panels) and $V_D = +20$ V, were applied for positive V_G (right panels). All devices were measured under atmospheric pressure N₂ at room temperature. Legend shows incident optical power density.

S4. Responsivity



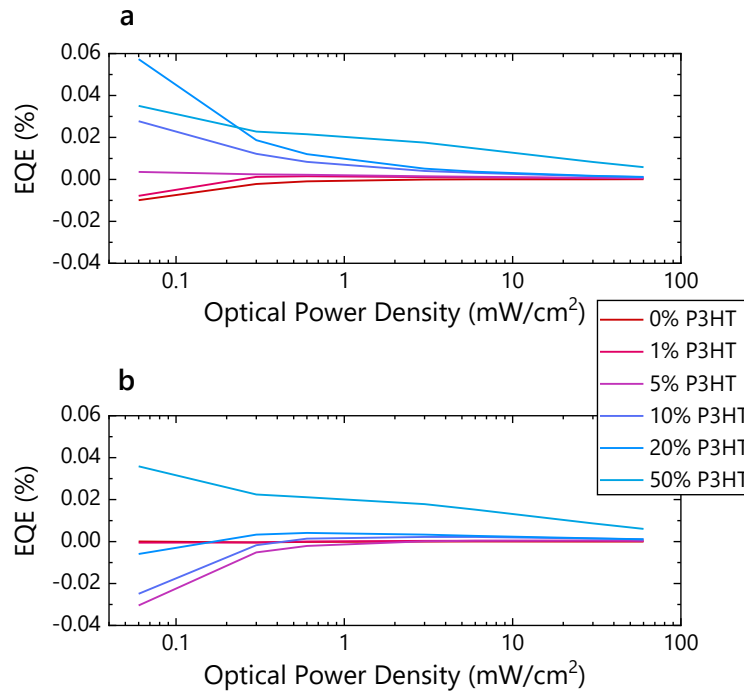
Supplementary Figure S4 Responsivity of phototransistors formed of blends of poly(3-hexylthiophene-2,5-diyl) (P3HT) and phenyl- C_{61} -butyric acid methyl ester (PCBM) with various weight % of P3HT, measured under various intensities of green ($\lambda_{\text{max}} = 525 \text{ nm}$) light. Responsivities were extracted with applied drain (V_D) and gate voltages (V_G) of **a** $V_D = -20 \text{ V}$ and $V_G = -20 \text{ V}$, **b** $V_D = 20 \text{ V}$ and $V_G = 20 \text{ V}$, **c** $V_D = -20 \text{ V}$ and $V_G = -100 \text{ V}$, **d** $V_D = 20 \text{ V}$ and $V_G = 100 \text{ V}$, respectively. Blue represents positive responsivities and red represent negative responsivities. All phototransistors measured were in the bottom-gate, bottom-contact (BGBC) architecture, as shown in Figure 1a of the main text and had a channel length of $20 \mu\text{m}$, a channel width of 1 cm , and a dielectric capacitance of 15 nF/cm^2 . All devices were measured under atmospheric pressure N_2 at room temperature.

S5. External Quantum Efficiency

External Quantum Efficiency (EQE) can be evaluated from responsivity via Equation S1:¹

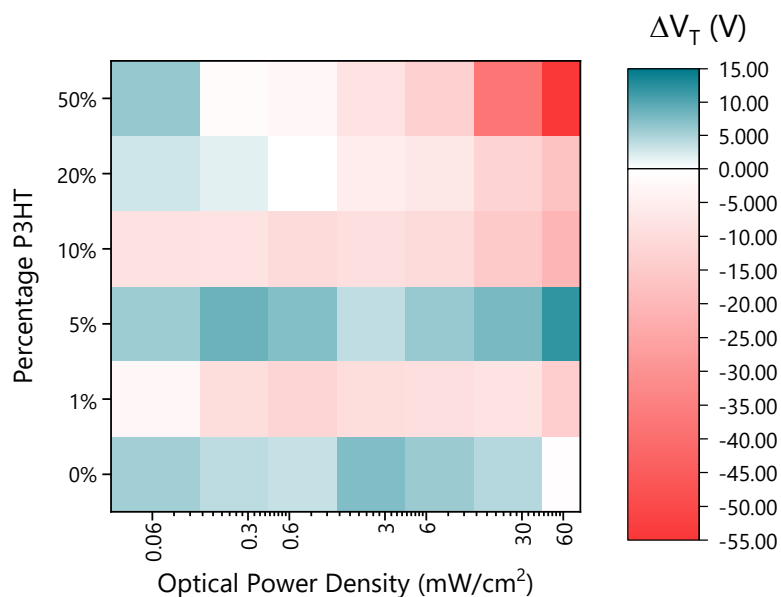
$$EQE = R \frac{hc}{e\lambda} = \frac{I_{ph}}{PLW} \frac{hc}{e\lambda} \quad (S1)$$

Here R is the responsivity, h is Planck's Constant, c is the speed of light *en vacuo*, e is the fundamental unit of charge, λ is the wavelength of incident photons (we here use the peak wavelength $\lambda = 525$ nm), I_{ph} is the photo-induced change in drain current under illumination ($I_{ph} = I_D^{(illuminated)} - I_D^{(dark)}$), P is the incident optical power density, L is the transistor channel length, and W is the transistor channel width. In Figure S5 the EQE is evaluated as a function of blend ratio and incident optical power density for applied voltages of **a** $V_D = -20$ V, $V_G = -20$ V and **b** $V_D = 20$ V, $V_G = 20$ V.



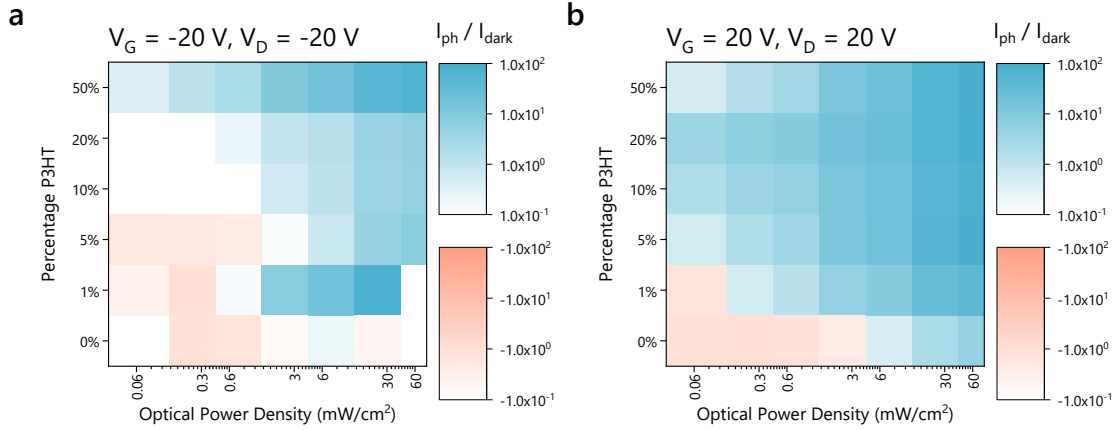
Supplementary Figure S5 External Quantum Efficiency (EQE) of phototransistors formed of blends of poly(3-hexylthiophene-2,5-diyl) (P3HT) and phenyl-C₆₁-butyric acid methyl ester (PCBM) with various weight % of P3HT, measured under various intensities of green ($\lambda_{max} = 525$ nm) light, evaluated using Equation S1. EQEs were extracted with applied drain and gate voltages of **a** $V_D = -20$ V and $V_G = -20$ V, and **b** $V_D = 20$ V and $V_G = 20$ V, respectively. All phototransistors measured were in the bottom-gate, bottom-contact (BGBC) architecture, as shown in Figure 1a of the main text and had a channel length of 20 μ m, a channel width of 1 cm, and a dielectric capacitance of 15 nF/cm². All devices were measured under atmospheric pressure N₂ at room temperature.

S6. Change in Threshold Voltage under Illumination



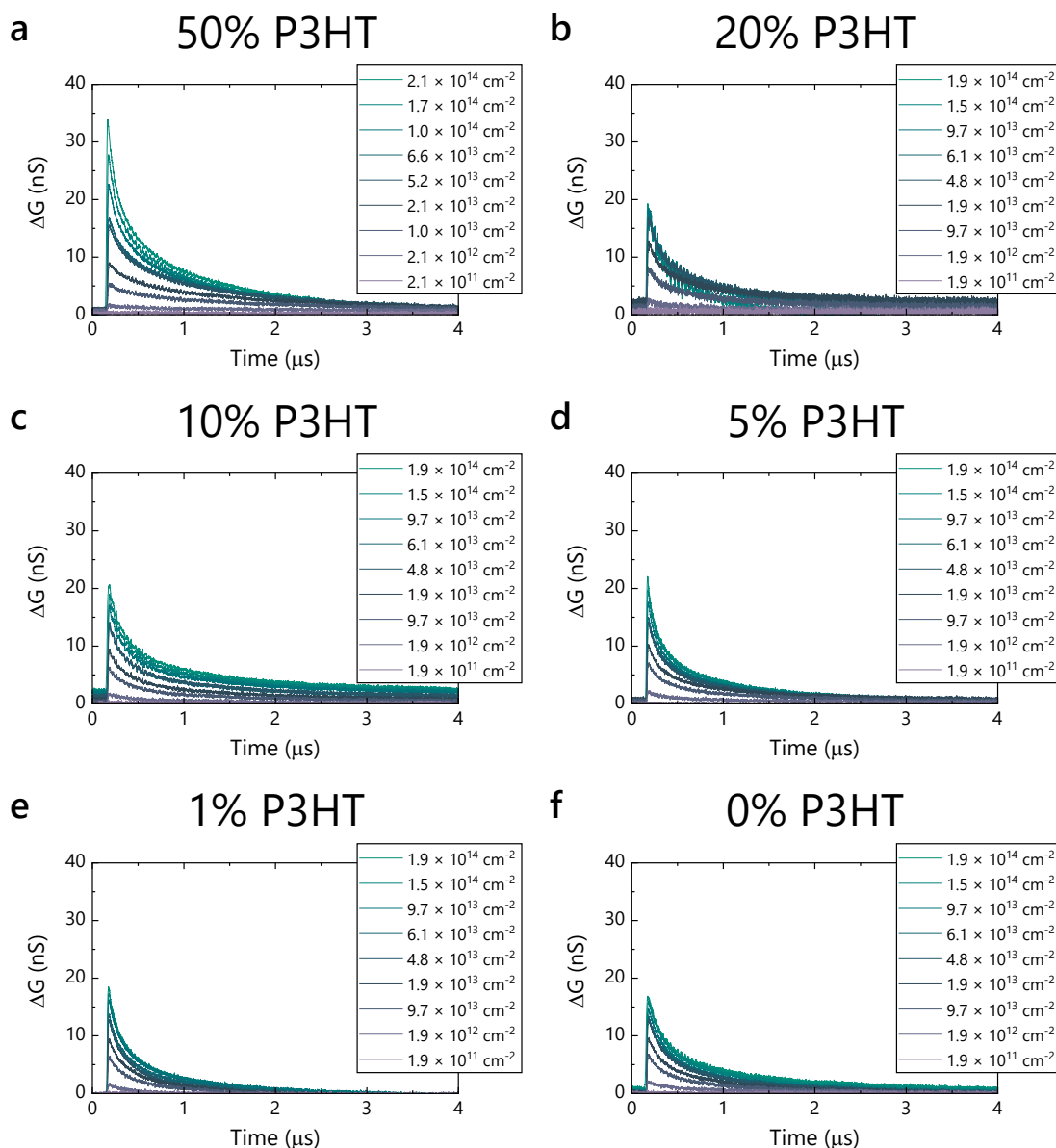
Supplementary Figure S6 Change in n-channel threshold voltage (ΔV_T) of phototransistors formed of blends of poly(3-hexylthiophene-2,5-diyl) (P3HT) and phenyl-C₆₁-butyric acid methyl ester (PCBM) with various weight % of P3HT, measured under various intensities of green ($\lambda_{\text{max}} = 525$ nm) light. ΔV_T was extracted with an applied drain voltage of $V_D = 20$ V. Green represents positive changes in V_T and red represent negative changes in V_T . All phototransistors measured were in the bottom-gate, bottom-contact (BGBC) architecture, as shown in Figure 1a of the main text and had a channel length of 20 μm , a channel width of 1 cm, and a dielectric capacitance of 15 nF/cm². All devices were measured under atmospheric pressure N₂ at room temperature.

S7. Ratio of Photocurrent to Dark Current

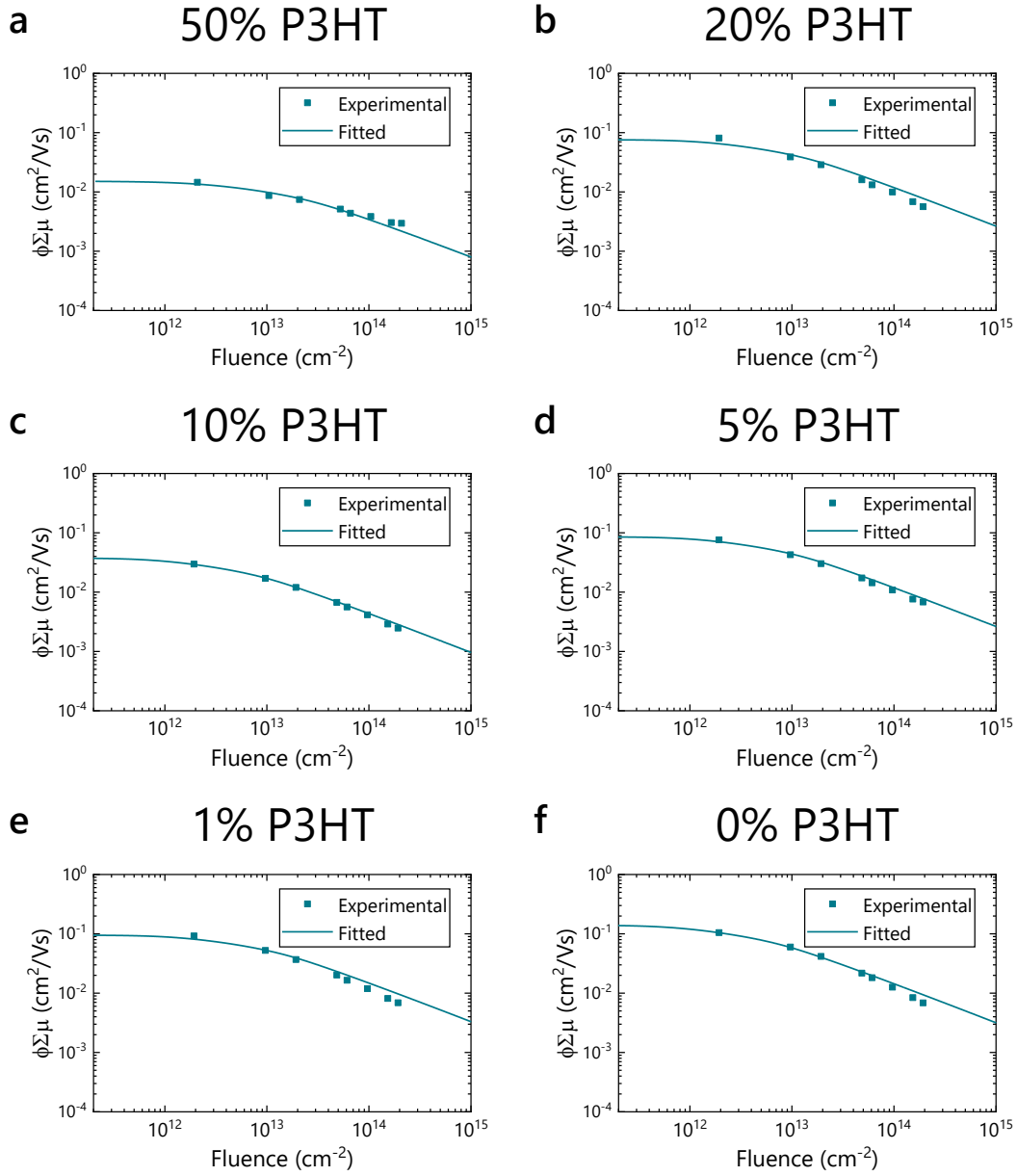


Supplementary Figure S7 Ratio of photocurrent ($I_{ph} = I_D^{(illuminated)} - I_D^{(dark)}$) to dark current ($I_D^{(dark)}$) for phototransistors formed of blends of poly(3-hexylthiophene-2,5-diyl) (P3HT) and phenyl-C₆₁-butyric acid methyl ester (PCBM) with various weight % of P3HT, measured under various intensities of green ($\lambda_{max} = 525$ nm) light. Ratios were extracted with applied drain (V_D) and gate voltages (V_G) of **a** $V_D = -20$ V and $V_G = -20$ V, **b** $V_D = 20$ V and $V_G = 20$ V, respectively. All phototransistors measured were in the bottom-gate, bottom-contact (BGBC) architecture, as shown in Figure 1a of the main text and had a channel length of 20 μ m, a channel width of 1 cm, and a dielectric capacitance of 15 nF/cm². All devices were measured under atmospheric pressure N₂ at room temperature.

S8. Time-Resolved Microwave Conductivity (TRMC) Data



Supplementary Figure S8 Photoconductance (ΔG) of blends of poly(3-hexylthiophene-2,5-diyl) (P3HT) and phenyl- C_{61} -butyric acid methyl ester (PCBM) as a function of time before, during, and after excitation from a green (532 nm) laser pulse. The weight % of P3HT was **a** 50%, **b** 20%, **c** 10%, **d** 5%, **e** 1%, **f** 0%. The fluence of the laser is provided in the legends. All measurements were carried out using time-resolved microwave conductivity (TRMC) in air at room-temperature. The laser pulse had a full width half-maximum (FWHM) of roughly 5 ns in all cases.



Supplementary Figure S9 TRMC figure of merit and proxy for carrier mobility, $\phi\Sigma\mu$, as a function of incident laser fluence for blends of poly(3-hexylthiophene-2,5-diyl) (P3HT) and phenyl-C₆₁-butyric acid methyl ester (PCBM). The weight % of P3HT was **a** 50%, **b** 20%, **c** 10%, **d** 5%, **e** 1%, **f** 0%. $\phi\Sigma\mu = \phi(\mu_e + \mu_h)$ where μ_e and μ_h are the average electron and hole mobilities measured over the sample area, respectively. ϕ is the carrier-generation efficiency, i.e. the number of electron-hole pairs generated per absorbed photon ($\phi \in [0,1]$). The points are experimental values and the lines are fits to a numerical model accounting for bimolecular and Auger recombination during the laser pulse.² All measurements were carried out using time-resolved microwave conductivity (TRMC) in air at room-temperature. The laser pulse had a full width half-maximum (FWHM) of roughly 5 ns in all cases.

Supporting References

- (1) Baeg, K.-J.; Binda, M.; Natali, D.; Caironi, M.; Noh, Y.-Y. Organic Light Detectors: Photodiodes and Phototransistors. *Adv. Mater.* **2013**, *25* (31), 4267–4295. <https://doi.org/10.1002/adma.201204979>.
- (2) Labram, J. G.; Chabinyk, M. L. Recombination at High Carrier Density in Methylammonium Lead Iodide Studied Using Time-Resolved Microwave Conductivity. *J. Appl. Phys.* **2017**, *122* (6), 065501. <https://doi.org/10.1063/1.4990802>.